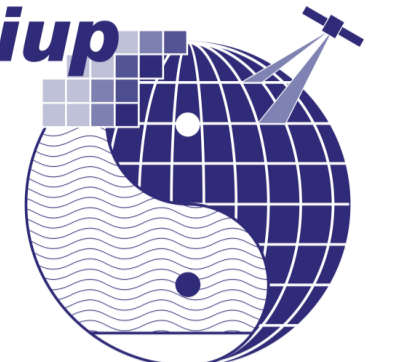
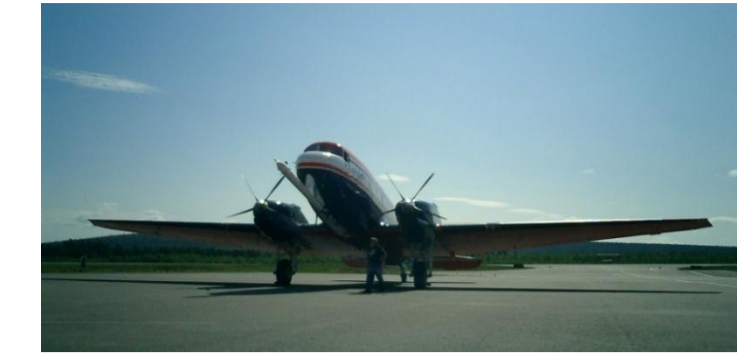


# Tropospheric trace gas mapping by airborne imaging DOAS

Anja Schönhardt\*, P. Altube, A. Richter, S. Krautwurst, K. Gerilowski, and J. P. Burrows

Institute of Environmental Physics, University of Bremen, Germany

\*Email: anja.schoenhardt@iup.physik.uni-bremen.de



## Objectives

**Objectives:** Measurements of tropospheric trace gases

→ NO<sub>2</sub> pollution mapping, identification of source regions and source strengths, satellite data validation, investigation of sub-pixel variability.

**Advantages of aircraft measurements and imaging DOAS**

- Higher spatial resolution ~100 m (down to <30 m) than satellite observations at useful spatial coverage
- Several viewing directions are observed at the same time, i.e. a broad stripe below the aircraft
- Less data is lost as cp. to scanning instruments, adjacent regions are viewed simultaneously

**History of the IUP Bremen iDOAS instrument:** development in 2011; laboratory measurements for optical characterisation; first test flights conducted during a flight campaign in summer 2011

## iDOAS in the Polar-5 aircraft

**Polar-5**

Registration: C-GAWI, Aircraft Type: Basler BT-67 / DC3

Length/Height/Span: 21 m / 5.2 m / 29 m

Speed & Altitude: 50-105 m/s; 100-19000 ft

Owner & Operator: AWI, Germany; Kenn Borek Air Ltd. Canada



Polar-5 in Hangar at Bremerhaven Lüneort airport



The IUP Bremen imaging DOAS instrument rack in the Polar-5 aircraft:

## Instrumental setup and viewing geometry

**Technical information and special features**

- Wide angle objective and fibre bundle (35 fibres) as entrance optics
  - Acton 300i imaging spectrometer, 600l/mm grating, blazed @500nm
  - Spectral window 415 - 455nm; 0.7-1.0nm resolution
  - Frame transfer (FT) CCD Detector, 512x512 pixels, 8.2x8.2 mm<sup>2</sup>
- Instrumental setup allows gap-free measurements (due to FT CCD) and flexible positioning in aircraft (due to sorted fibre bundle).

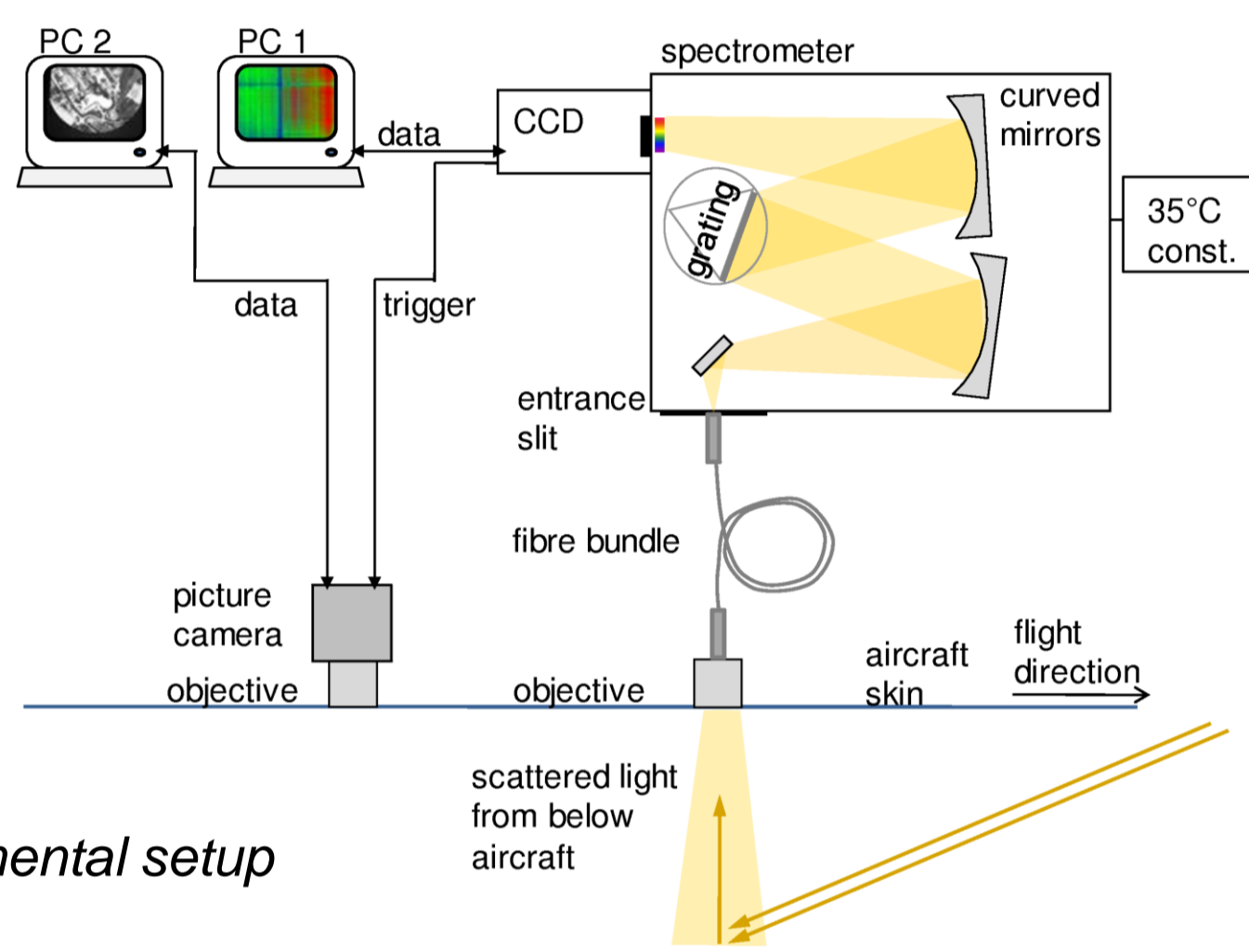


Fig. 1: Instrumental setup

**Observation and viewing geometry**

- Two nadir ports: spectrometer objective and picture camera
- Geolocation information: from GPS sensor and gyrometer
- Viewing directions: max. 35 LOS (line of sight) from 35 fibres
- LOS after averaging across track: fibres combined to 9 LOS (θ)
- Field of view: ~48° across track (γ), ~3° along track (θ)
- Swath width: on the order of flight altitude H
- Exposure time t<sub>exp</sub>: typ. 0.5s
- Spatial resolution: ~100 m (at 1km flight altitude, 9 viewing directions, depending on flight altitude and required SNR)

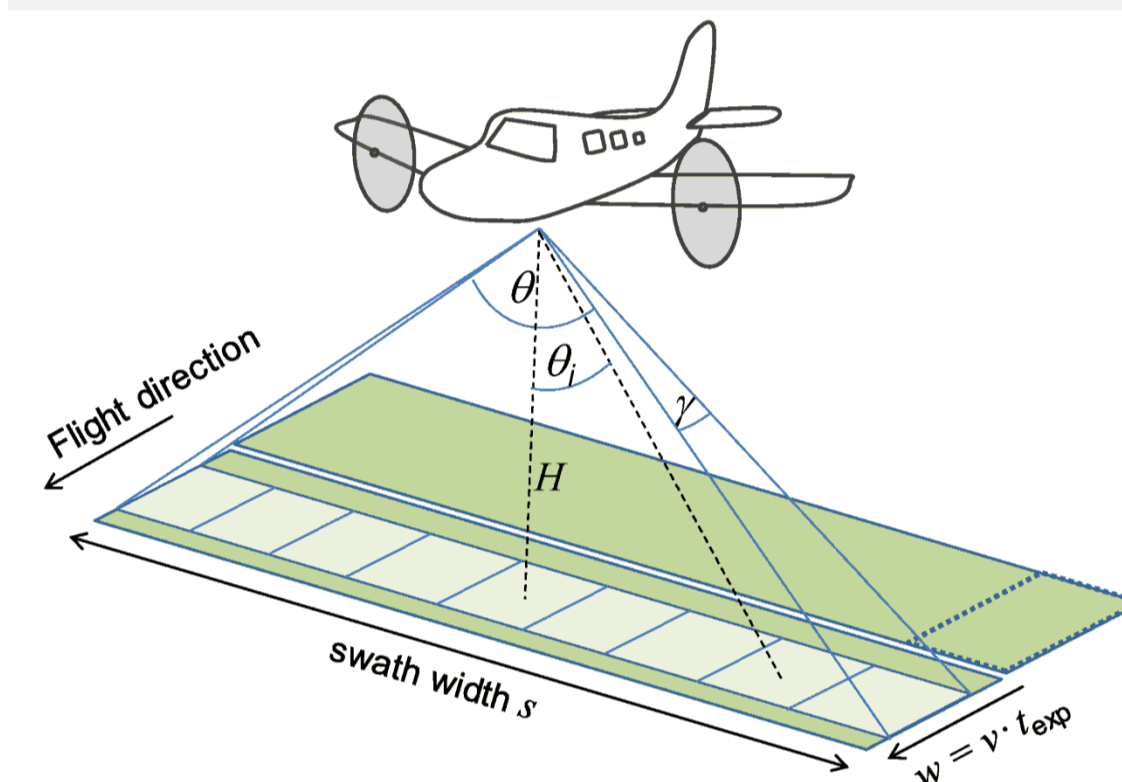
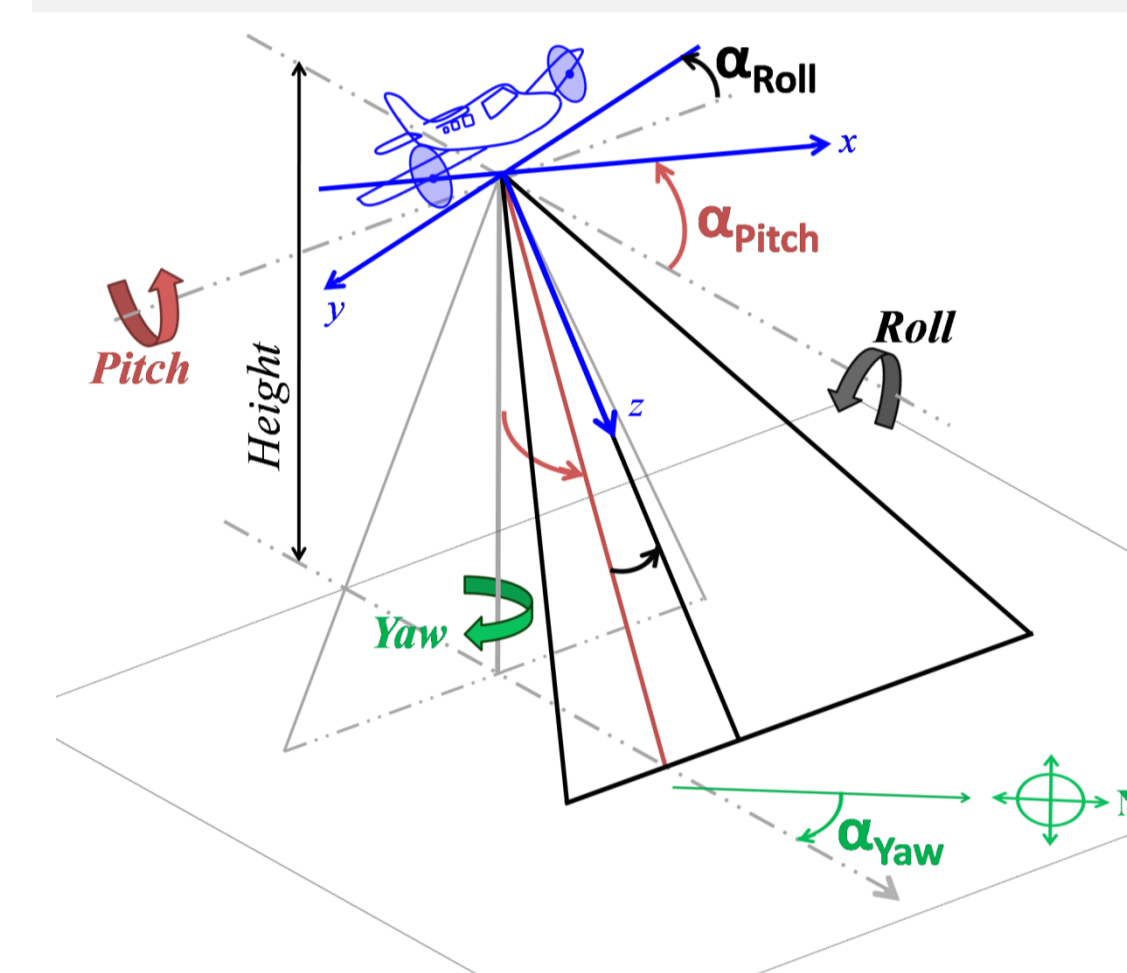


Fig. 2: Sketch of the iDOAS viewing geometry

- single spatial pixel
- observed area (FOV)
- instantaneously observed area (iFOV)

**Computation of viewing geometry in flight**

- Calculation of correct ground geolocation is important
- Consideration of the aircraft angles (pitch, roll and yaw) is required in addition to GPS position
- Corner coordinates and pixel center for each LOS calculated for start and end of exposure to determine the pixel area
- The displacements of the ground pixel due to aircraft motions can be significant (depending on flight altitude)



**Displacements**

- During straight tracks: few tens of metres
- During turns: order of 500m, max. ~1km

Fig. 3: Sketch of the aircraft angles affecting the observed area on the ground

## NO<sub>2</sub> vertical columns and emission flux calculations above a power plant

**NO<sub>2</sub> retrieval above a power plant**

- Black coal power plant (848 MW) at Ibbenbüren (52° 17.2' N, 7° 44.8' E)
- Slant columns of NO<sub>2</sub> retrieved by Differential Optical Absorption Spectroscopy
- Large variation of NO<sub>2</sub> amounts across and along track are observed
- The NO<sub>2</sub> in the exhaust plume downwind of the power plant is clearly visible

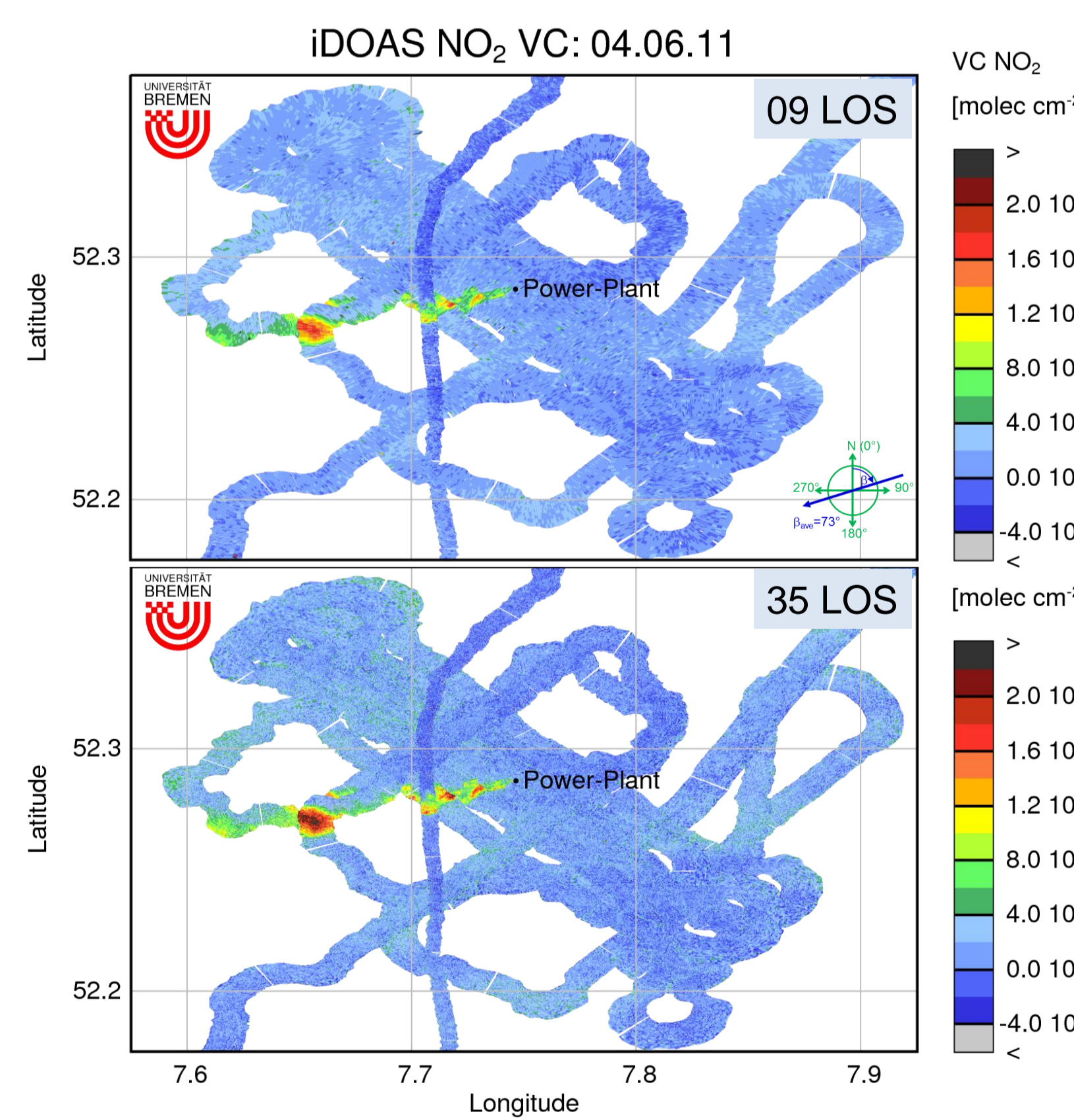


Fig. 4: NO<sub>2</sub> amounts along the flight track retrieved from the flight on 04.06.2011. Downwind from the power plant of Ibbenbüren, strong enhancement of NO<sub>2</sub> is visible (average wind direction was about East North-East, see inset). Enhanced NO<sub>2</sub> is on the order of 10<sup>16</sup> molec/cm<sup>2</sup>. Top: Division of the field of view into 9 lines of sight (LOS) allowing spatial resolution of ~100m. Bottom: Consistent result for full spatial resolution of 35 LOS with ground pixel side length on the order of ~30m. Fine spatial variability of NO<sub>2</sub> amounts is resolved.

**Retrieval Settings**

**Fitting window:** 425 – 450 nm

**Trace gases:**

NO<sub>2</sub> (293K), O<sub>3</sub> (241K), O<sub>4</sub> (296K), H<sub>2</sub>O (HITRAN)

**Atmospheric effects:**

Ring (SCIATRAN calculated), intensity offset

**Polynomial:** quadratic

**Reference I<sub>0</sub>:** rural scene from same LOS

**Slit function:** individual for each LOS

**Detection Limit for NO<sub>2</sub>**

Slant Column detection limit ~10<sup>15</sup> molec/cm<sup>2</sup>; optical density rms on the order of 10<sup>-3</sup>

**Air mass factors, AMF (SCIATRAN)**

Rayleigh atmosphere, 1 km NO<sub>2</sub> box profile, 5% albedo, SZA and LOS dependence.

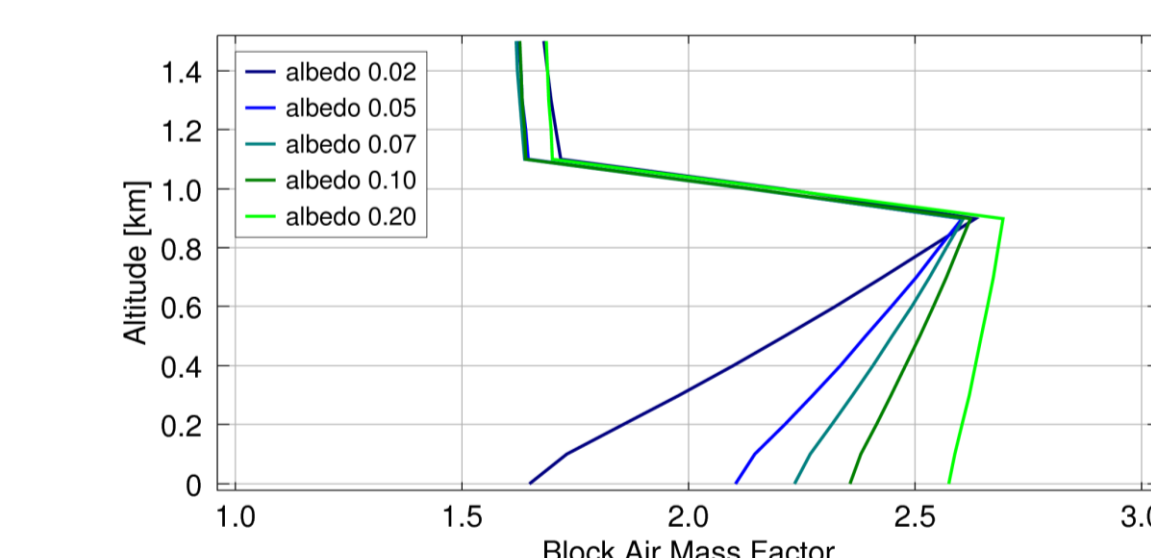


Fig. 5: Block AMF for different albedos at 40° SZA and a flight altitude of 1.1 km. AMF differences between box profile and elevated gaussian plume depend on altitude (example cases ~10% effect).

**NO<sub>2</sub> emission flux calculations**

- based on Gaussian plume dispersion model
- mean wind speed & direction determined from NO<sub>2</sub> profile (Gaussian shape, cp. Fig.6) using COSMO-DE model wind data
- Flux calculations performed at different distances from stack

$$c(x, y, z) = \frac{Q}{2\pi\sigma_y\sigma_z u} \exp\left(-\frac{y^2}{2\sigma_y^2}\right) \exp\left(-\frac{z^2}{2\sigma_z^2}\right) \quad \text{Eq. 1: Gaussian distribution of concentration } c$$

Dispersion of concentration  $c$  across plume ( $y$ ) and over altitude ( $z$ ) is taken into account, with source strength  $Q$ , wind speed  $u$  and spread  $\sigma_y$  and  $\sigma_z$ . Along the wind direction  $x$  only advection is considered.

$$Q \cong \int VC \cdot \vec{u} \cdot d\vec{l} \approx \sum_i VC_i \cdot \vec{u} \cdot d\vec{l}_i \quad \text{Eq. 2: Derived using Gaussian divergence theorem}$$

Approximation of source strength is achieved via discrete sum over the product of vertical columns ( $VC$ ), wind speed and path length  $d\vec{l}$ .

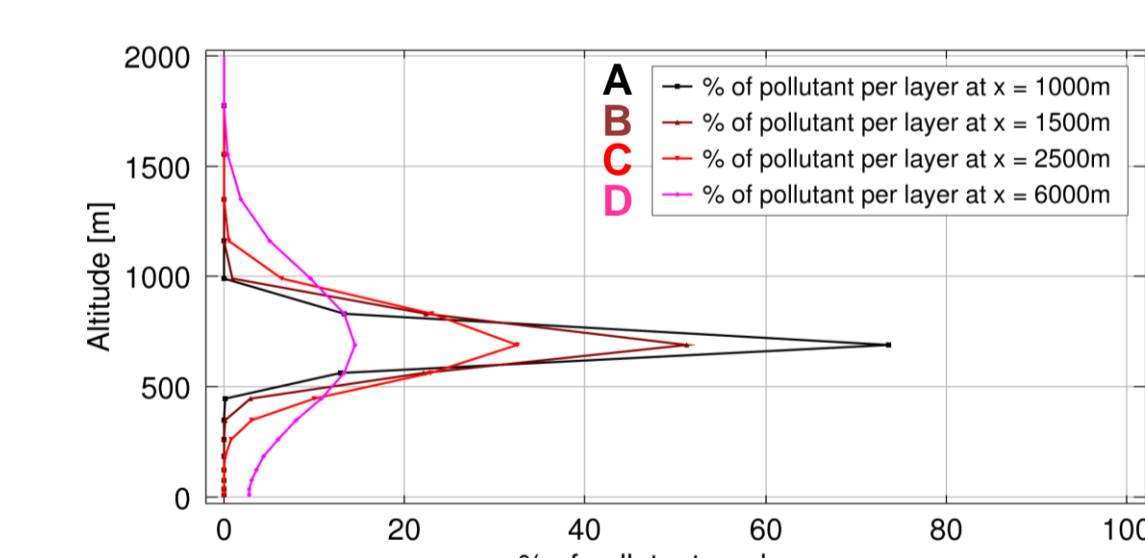


Fig. 6: Relative NO<sub>2</sub> altitude distribution inside the plume at three different distances from the stack. The profiles are used to determine mean wind speed and direction.

**Estimated emissions of NO<sub>2</sub>:**  
E<sub>NO<sub>2</sub></sub> ~ 2100-2400 T/a  
**Emissions of NO<sub>x</sub>**  
Using factor NO/NO<sub>2</sub> = 1/4:  
E<sub>NO<sub>x</sub></sub> ~ 2635-3000 T/a (good agreement with E-PRTR)

## NO<sub>2</sub> above inhabited and rural areas

**Flight on 09.06.2011**

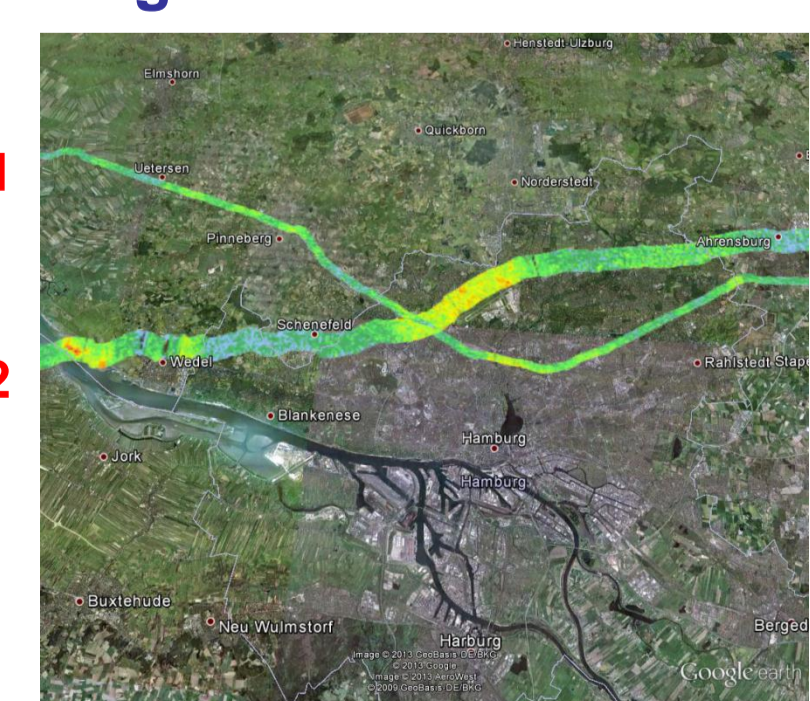


Fig. 7: NO<sub>2</sub> observations during two overflights over the city of Hamburg (same colour scale as Figs. 4 & 9.)

**Hamburg:**

- NO<sub>2</sub> maxima ~1-2·10<sup>16</sup> molec/cm<sup>2</sup>
- Enhanced NO<sub>2</sub> above the city and close to the airport
- Strong spatial variability

**Rural areas:**

NO<sub>2</sub> overall much lower than closer to cities  
Not all NO<sub>2</sub> enhancements can be assigned to local sources → transported NO<sub>2</sub> is observed.

**Fig. 8: Flight altitude on 09.06.2011**

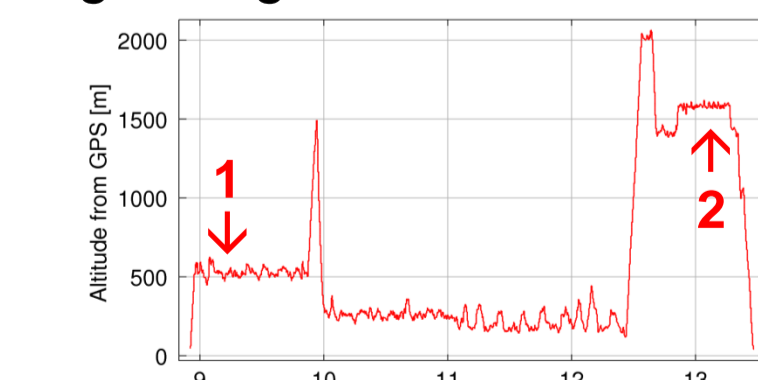


**Fig. 9: NO<sub>2</sub> vertical columns observed on 09.06.2011**

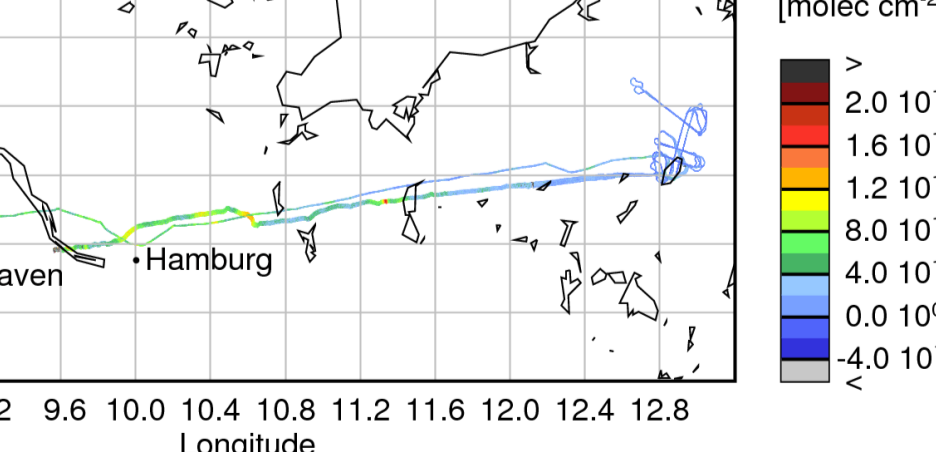


Fig. 9: NO<sub>2</sub> vertical columns observed on 09.06.2011

## Summary and Outlook

**Summary**

- Imaging DOAS instrument shows good imaging quality and good performance for NO<sub>2</sub> measurements
- Aircraft pitch, roll and yaw angles are fully taken into account for correct ground geolocation
- NO<sub>2</sub> column amounts have been retrieved, pollution sources are observed
- NO<sub>2</sub> emission fluxes are calculated for power plant point source
- Further observations: large spatial NO<sub>2</sub> variability, consistent low NO<sub>2</sub> above rural areas, transported NO<sub>2</sub>

**Activities for the future**

- Air mass factor consideration will be improved in future analyses
- Further dedicated campaigns will be conducted

**Selected References**

- P.Wang, et al: Measurements of tropospheric NO<sub>2</sub> with an airborne multi-axis DOAS instrument, Atmos. Chem. Phys., 5, 337–343, 2005.
- F. Lohberger, et al.: Ground-based imaging differential optical absorption spectroscopy of atmospheric gases, Vol. 43, No. 24, Applied Optics, 2005.
- K.-P. Heue, et al.: Direct observation of two dimensional trace gas distributions with an airborne Imaging DOAS instrument, Atmos. Chem. Phys., 8, 6707–6717, 2008.
- C. Popp et al.: High-resolution NO<sub>2</sub> remote sensing from the Airborne Prism Experiment (APEX) imaging spectrometer, Atmos. Meas. Tech., 5, 2211–2225, 2012.

**Acknowledgements**

The authors gratefully acknowledge financial support by the University of Bremen and by ESA through the TIBAGS project. Campaign support from AWI Bremerhaven, Martin Gehrman and Franziska Nehring, is gratefully acknowledged. Thank you to the aircraft crew from Kenn Borek, Canada.